

University of *Ljubljana*  
Faculty of *Mathematics and Physics*



Department of Physics

Seminar

# Raman spectroscopy for medical diagnostics

Author: Peter Naglič

Advisor: prof. dr. Boris Majaron

Date: May 2012

## Abstract

Raman spectroscopy is based on analysis of inelastically scattered light. This technique has a wide range of uses in chemistry, solid-state physics and other fields. Raman spectroscopy can distinguish between molecules and can identify them by their characteristic spectra. In this seminar I will discuss instrumentation required for Raman spectroscopy in medical applications, followed by specifics of data processing. At the end, I will present two examples of Raman spectroscopy used in medical diagnostics for detection of breast and skin cancer.

# Contents

<b>1</b>	<b>Introduction</b>	<b>2</b>
<b>2</b>	<b>Fundamentals of Raman spectroscopy</b>	<b>3</b>
2.1	Basic theory . . . . .	3
<b>3</b>	<b>Instrumentation</b>	<b>6</b>
3.1	Excitation source . . . . .	6
3.2	Sample illumination and light collection system . . . . .	6
3.3	Detection system . . . . .	7
<b>4</b>	<b>Data pre-processing</b>	<b>8</b>
4.1	Spectral calibration . . . . .	8
4.2	Elimination of fluorescence . . . . .	8
4.3	Analysis of Raman spectra . . . . .	9
<b>5</b>	<b>Clinical applications of Raman spectroscopy</b>	<b>9</b>
5.1	Skin cancer diagnostics . . . . .	10
5.2	Breast cancer diagnostics . . . . .	11
<b>6</b>	<b>Conclusion</b>	<b>14</b>
	<b>References</b>	<b>14</b>

## 1 Introduction

Light can interact with matter in many different ways and its response can yield useful information about the properties of the material. A good feature of light is non-invasive probing of the material, when it is used at low intensities. This is especially important when we deal with human tissue. Another advantage is real time data acquisition and processing. The diagnosis can be made on the spot.

When light is incident upon a material, it can in general be reflected, absorbed, scattered or transmitted. There are various techniques based on these different light-material interactions: absorption spectroscopy, reflectance spectroscopy, fluorescence spectroscopy and Raman spectroscopy. Each of these techniques has its advantages and disadvantages.

Raman spectroscopy has a wide range of uses. It is very common in chemistry, where different molecules can be identified by their characteristic bond vibrations. Raman spectroscopy can be used to analyze gas mixtures or detect explosives. In solid-state physics, Raman spectroscopy is used to characterize materials, measure temperature, or get the information about crystal orientation. Because this technique can identify and distinguish between molecules, it has found its use in biomedicine, especially in tissue diagnostics.

In this seminar I will focus on Raman spectroscopy and its clinical applications. When certain tissue starts to transform (e.g., cancerous cells begin to develop), its chemical composition often changes. If this change can be detected using Raman spectroscopy, the correct diagnosis can be made in early stage of the disease. At the beginning of the seminar I will explain the basics of Raman spectroscopy. Then I will move on to instrumentation and how we acquire the measurements. This will be followed by data processing, analysis and how a diagnosis can be made. At the end I will present two application examples, detection of breast and skin cancer.

## 2 Fundamentals of Raman spectroscopy

Raman spectroscopy is based on analysis of inelastically scattered light. This type of scattering is named after its discoverer Sir Chandrasekhara Venkata Raman. Since there were no lasers at that time, Raman used focused sunlight, a narrow band photographic filter to make the sunlight monochromatic, dust-free vapour to scatter the monochromatic light and another filter to block the unscattered light. He found that a small amount of light had changed the frequency and passed through the second filter. For this discovery Raman received the Nobel Prize in physics in 1930 [1]. Since the introduction of lasers, the sensitivity of Raman spectroscopy has greatly enhanced. It has become a significant field in spectroscopy in general.

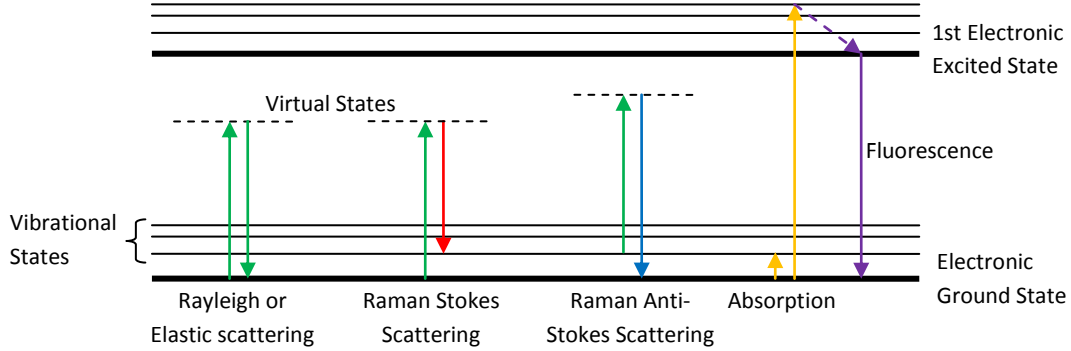


Figure 1: Energy level diagram for Rayleigh and Raman scattering.

### 2.1 Basic theory

In Raman spectroscopy, a sample is irradiated by a laser beam and the scattered light is observed. Rayleigh or elastic scattered light has the same frequency as incident light and is relatively strong. Raman or inelastic scattered light has a frequency different from that of the incident light and is very weak ( $10^{-5}$  of the intensity of the incident beam [2]). Raman scattering can be regarded as inelastic collision of an incident photon with a molecule, Fig. 1. The molecule is excited to a virtual state and after the interaction, the energy of the outgoing photon is different from the energy of the incident photon, and the molecule is found in either a higher or lower vibrational state. If the energy of the outgoing photon is lower than the energy of the incident photon ( $\hbar\omega_s < \hbar\omega_0$ ), the process is referred to as Stokes scattering. The process in which the outgoing photon has higher energy ( $\hbar\omega_{as} > \hbar\omega_0$ ) is called anti-Stokes scattering. Anti-Stokes scattering requires molecules to already be in a higher vibrational states. Therefore, the intensity of the Stokes scattered light is higher since the population of molecules in lower vibrational states is larger, according to Maxwell-Boltzmann distribution law.

Classical description of Raman scattering [2] starts from relation for induced electric dipole moment

$$\mathbf{p}_{ind} = \alpha \mathbf{E}, \quad (1)$$

where  $\alpha$  is polarizability of a molecule and  $\mathbf{E}$  is electric field strength. In the electromagnetic wave,  $\mathbf{E}$  fluctuates with time as

$$\mathbf{E} = \mathbf{E}_0 \cos(\omega_0 t). \quad (2)$$

If the molecule is vibrating, the normal coordinates of nuclear displacements  $q_n(t)$  can be approximated for small amplitudes by

$$q_n(t) = q_{n0} \cos(\omega_n t), \quad (3)$$

where  $q_{n0}$  and  $\omega_n$  denote the amplitude and vibrational frequency of the  $n$ -th normal vibration, respectively. Here we have also assumed the adiabatic approximation, where the electronic charge distribution of a molecule adjusts “instantaneously” to changes in nuclear positions. Complex vibrations of larger molecules with many atomic nuclei can be expressed as a superposition of normal vibrations, which are mutually independent. In a  $N$ -atom molecule there are  $3N-6$  normal vibrations. For linear molecules this becomes  $3N-5$ , since rotation about the molecular axis cannot be observed.

For small amplitudes of vibration, polarizability can be expanded to the linear term in  $q_n(t)$  via Taylor series. Thus, we can write

$$\alpha = \alpha_0 + \sum_{n=1}^{3N-6} \left( \frac{\partial \alpha}{\partial q_n} \right)_0 q_n + \dots \quad (4)$$

Here,  $\alpha_0$  is the polarizability at the equilibrium position and  $(\partial \alpha / \partial q_n)_0$  the rate of change of  $\alpha$  with respect to  $q_n$ , evaluated at the equilibrium position. Inserting (4) into (1) yields the induced dipole moment

$$\begin{aligned} \mathbf{p}_{ind}(t) &= \alpha_0 \mathbf{E}_0 \cos(\omega_0 t) + \mathbf{E}_0 \sum_{n=1}^{3N-6} \left( \frac{\partial \alpha}{\partial q_n} \right)_0 q_{n0} \cos(\omega_n t) \cos(\omega_0 t) \\ &= \alpha_0 \mathbf{E}_0 \cos(\omega_0 t) + \frac{\mathbf{E}_0}{2} \sum_{n=1}^{3N-6} \left( \frac{\partial \alpha}{\partial q_n} \right)_0 q_{n0} [\cos \{(\omega_0 + \omega_n)t\} + \cos \{(\omega_0 - \omega_n)t\}]. \end{aligned} \quad (5)$$

According to the classical theory the first term represents an oscillating dipole which radiates light at frequency  $\omega_0$  (Rayleigh scattering), while the second term describes Raman scattering. Vibrations that lead to the Raman effect are called Raman active. As we can instantly see, if  $(\partial \alpha / \partial q_n)_0 = 0$ , the corresponding normal vibration is not Raman active.

In relation to Raman activity, we have to look more carefully at the polarizability,  $\alpha$ . In general,  $\alpha$  is a tensor of rank two, because the response of the molecule is not the same in every direction with respect to the electric field. The tensor is symmetric. For small molecules it is easy to see whether the polarizability changes during the vibration. If we consider a linear molecule, such as  $\text{CO}_2$ , the electrons are more polarizable (a larger  $\alpha$ ) along the chemical bond than in the direction perpendicular to it. It is convenient to plot  $1/\sqrt{\alpha_i}$ , where  $\alpha_i$  is the principal value of the tensor. We end up with a polarizability ellipsoid. If the size, shape or orientation of this ellipsoid changes during a certain normal vibration, the latter could be Raman active. Fig. 2a shows the changes of the ellipsoid for two normal vibrations. Vibration  $\nu_1$  is Raman active, because the polarizability is changing in every direction (see Fig. 2b). Although the ellipsoid is also changing during the vibration  $\nu_3$ , the change occurs symmetrically with respect to  $q$  and therefore  $(\partial \alpha / \partial q_n)_0 = 0$ .

A Raman spectrum is a plot of intensity of the scattered light as a function of frequency shift between the incident and scattered photons. The frequency shift is usually presented in “wavenumbers”, defined as

$$\Delta \tilde{\nu} [\text{cm}^{-1}] = \frac{1}{\lambda} = \frac{\Delta E}{hc}, \quad (6)$$

where  $\Delta E$  denotes the energy difference between the initial and final vibrational state of the

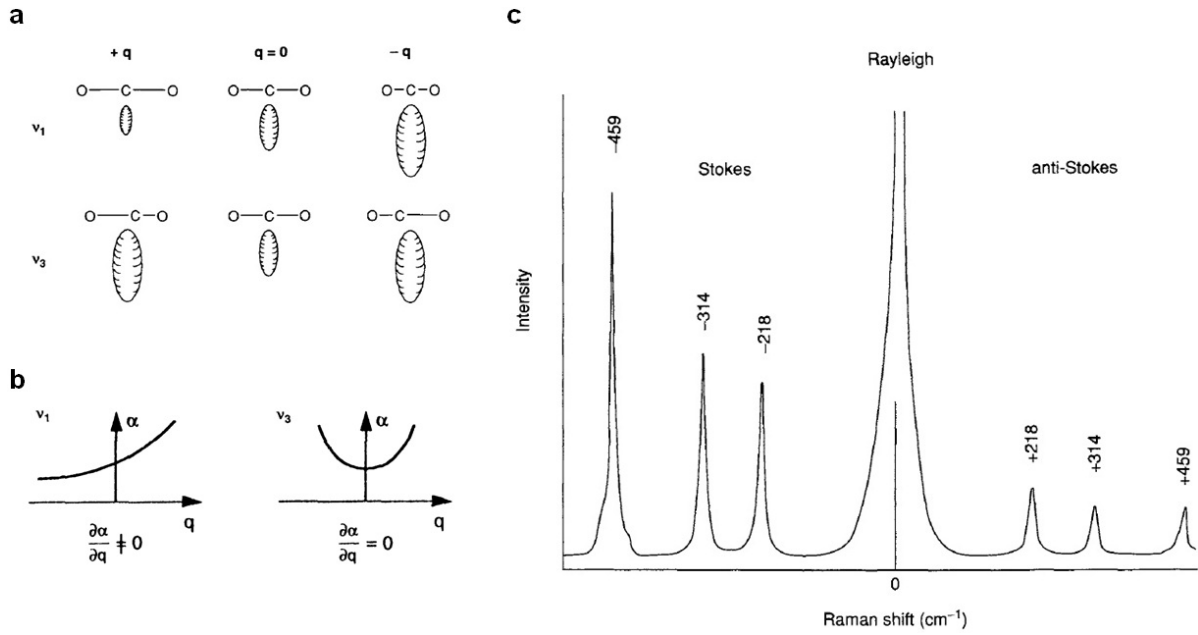


Figure 2: (a) Changes in polarizability ellipsoid during two normal vibrations of CO<sub>2</sub> molecule. (b) Polarizability of a CO<sub>2</sub> molecule as a function of vibration coordinate  $q$ . (c) Raman spectrum of CCl<sub>4</sub>. The intensity is given in a logarithmic scale. [2]

molecule.

The Raman frequency shift is mostly observed in the  $10^2 - 10^4 \text{ cm}^{-1}$  region. For example, near-infrared excitation light with a wavelength of 830 nm is equivalent to  $12048 \text{ cm}^{-1}$ . If we have a typical Stokes shift of  $-1000 \text{ cm}^{-1}$ , the outgoing photon has energy of  $11048 \text{ cm}^{-1}$ , which is equivalent to 905 nm. In each spectrum, the peaks are characteristic for normal vibrations of each molecule. This actually works as a “fingerprint” and we can identify which molecules are present in a chemical compound. Fig. 2c shows a typical Raman spectrum of CCl<sub>4</sub>. The intensity of the Stokes lines is usually a few orders of magnitude larger than for anti-Stokes. Because the peaks occur symmetrically with respect to the frequency of the incident light, it is sufficient to only acquire the Stokes lines.

### 3 Instrumentation

Raman spectroscopy setup consists of three main components:

- excitation source (a laser)
- sample illumination and light collection system
- detection system

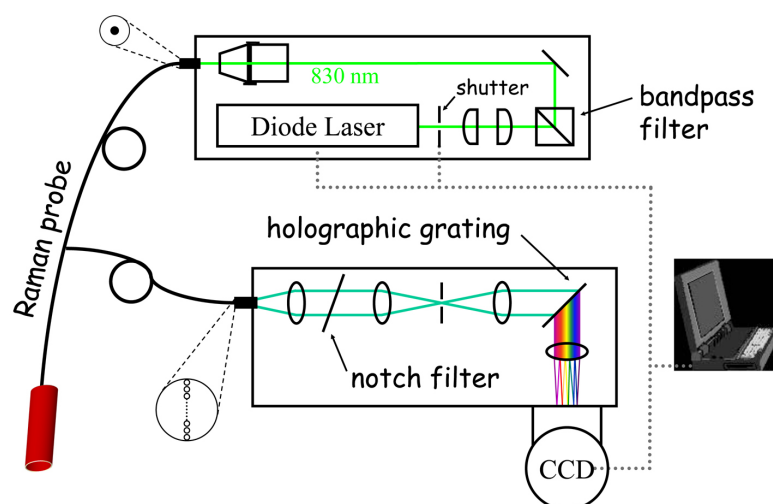


Figure 3: Scheme of a typical setup for NIR dispersive Raman spectroscopy. [10]

#### 3.1 Excitation source

In this seminar I will mostly discuss near-infrared (NIR) dispersive Raman spectroscopy. This technique uses NIR radiation as excitation source that stretches from 780 to 1100 nm. The main advantage of this wavelength region is the reduction of fluorescence, thus making detection of the weak Raman signal easier.

After the invention of lasers, Ti:Sapphire laser was mostly used for NIR Raman spectroscopy. Ti:Sapphire laser is useful because of its high output power, single-wavelength mode operation and Gaussian beam profile. However, because of its size and cooling requirements, this system is not practical for use in portable clinical systems.

With the introduction of diode lasers, portable Raman spectroscopy setups started to appear. Diode lasers are small ( $< 1 \text{ mm}^3$ , [2]), have high efficiency and are easily cooled. The main disadvantage of diode lasers is the wavelength drift due to the change of the temperature. It is therefore necessary to stabilize the wavelength mode by controlling the temperature to within  $\pm 0.01^\circ\text{C}$ . Such diode lasers are optimized and manufactured specifically for Raman spectroscopy.

#### 3.2 Sample illumination and light collection system

Since Raman scattering signal is weak, the laser beam must be properly delivered onto the sample, and the scattered light efficiently collected. For practical reasons light is typically delivered and collected using optical fibers made of silica. However, many molecules, including silica, are themselves Raman active, so the Raman signal from silica can interfere with the sample signal. Such unwanted fiber signal can be generated both in the delivery fiber, by the

excitation light, and in collection fibers by light elastically scattered from the sample. This problem can be solved using a bandpass filter at the end of the delivery fiber, transmitting only excitation light, and a long-pass or notch filter in front of the collection fiber, blocking the Fresnel reflected and elastically scattered laser light. Filters can be included in a special Raman probe for compact design (Fig. 4).

Besides above mentioned factors, the probe size and structure have to be appropriate for clinical use. It has to withstand pressure, temperature variations and contacts with various tissues and chemicals for disinfection.

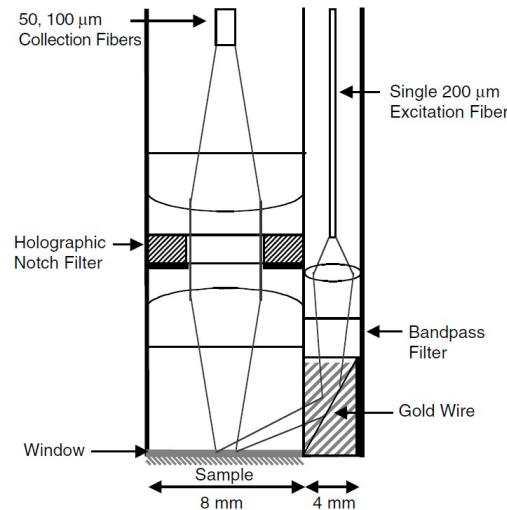


Figure 4: An example of a Raman probe for endoscopy.[3]

### 3.3 Detection system

Before the invention of lasers and highly sensitive detectors, Raman spectroscopy was struggling as a technique because of the low intensity of the Raman scattered light. Detection system consists of a suitable spectrometer and usually a CCD (charged coupled device). Spectrometer mostly uses a holographic grating and should ideally be compact and portable. A CCD camera consists of a rectangular chip or often just a linear CCD array, where the horizontal axis corresponds to wavelength. The vertical axis is used to stack signals from multiple fibers, which are commonly binned for improved signal-to-noise ratio. To about 1100 nm, the detectors are mostly silicon based, but for longer wavelengths other types are used, such as InGaAs (indium gallium arsenide) and Ge (germanium). The most important feature of these detectors is the speed of acquisition, which should be as short as possible in clinical use. Due to dark current and read-out noise, the CCD detector has to be cooled down to about  $-80^{\circ}\text{C}$ . Most effective and compact are multi-stage Peltier cooling systems, which can replace liquid nitrogen cooling. CCDs have high quantum efficiency (in the order of 90%) in the near infrared.

## 4 Data pre-processing

Before analysis Raman spectra must be pre-processed, e.g. spectral calibration, noise smoothing, and elimination of fluorescence.

### 4.1 Spectral calibration

Since there is a variety of Raman spectroscopy setups, where each uses a slightly different approach, a standard must be set, so that the data obtained can be transferred and compared. The horizontal axis of the CCD chip, which corresponds to wavelength, has to be calibrated using a known source such as a neon lamp. The efficiency of components in a Raman spectrometer is usually wavelength-dependent. This includes the grating, filters, optical elements in general, and the quantum efficiency of the CCD chip. Therefore, the wavelength dependence of the system response must be calibrated. This is usually done by a standard NIST-calibrated source such as a tungsten lamp to generate the correction factors. For intensity calibration, the Raman spectra of several well known Raman scatterers are used. These include naphthalene, rhodamine 6G, methylene blue, etc. Finally, the wavelength of the excitation laser needs to be taken into account, because the spectrum is given in relative wavenumbers in respect to the laser wavelength.

### 4.2 Elimination of fluorescence

Complex molecules in the sample and impurities in the optical elements can absorb the laser radiation and emit a fluorescence signal. When this occurs, Raman spectrum can be obscured by a broad and strong fluorescence band. This fluorescence is often orders of magnitude more intense than the weak Raman signal. There are several ways to minimize the fluorescence. Hardware solutions use wavelength shifting of the excitation laser or time gating, which are effective, but they require modifications to the experiment setup. Mathematical methods are usually a better solution. These include first-order differentiation, fast Fourier transform, and polynomial fitting.

The first derivative approach involves measuring the spectrum at two slightly shifted excitation wavelengths. The fluorescence remains unchanged at both excitation wavelengths, whereas the Raman peaks are shifted. Integrating the difference of the two spectra gives the Raman spectrum.

Alternatively, one can record the spectrum only at a single excitation wavelength, take the first derivative and integrate after noise smoothing and baseline correction of the spectrum derivative. However, this method can severely distort the Raman line shapes.

With fast Fourier transformation, the measured spectrum can be transformed to the frequency domain. The FFT of the signal can be multiplied with a linear filter that cuts the low frequency components to eliminate the slowly changing fluorescence baseline. The inverse FFT then yields the Raman spectrum. This method can cause artefacts in the processed spectra, if the frequency components of the Raman signal and fluorescence are not well separated.

The third and probably the most accurate method is to fit a polynomial (usually of fourth or fifth order) to the measured spectrum. In this case, the slow baseline of the fluorescence is taken into account, leaving out the fast changing Raman line shapes. The automated polynomial fitting is named modified-mean method. The basis of this method is a single sliding-averaging filter, in which the centre pixel in the window is set equal to the mean of all intensities in the window. If that pixel has higher intensity after the filtering, it is reassigned back to its original value. Eventually, this gives the underlying shape of the baseline fluorescence, which is fitted with a polynomial and subtracted from the original spectrum. The result is a Raman spectrum



free of fluorescence.

Fig. 5 shows the effectiveness of three software methods for removal of the fluorescence signal. Each of these methods has its advantages and disadvantages, but the most effective is usually polynomial fitting (heavy line).

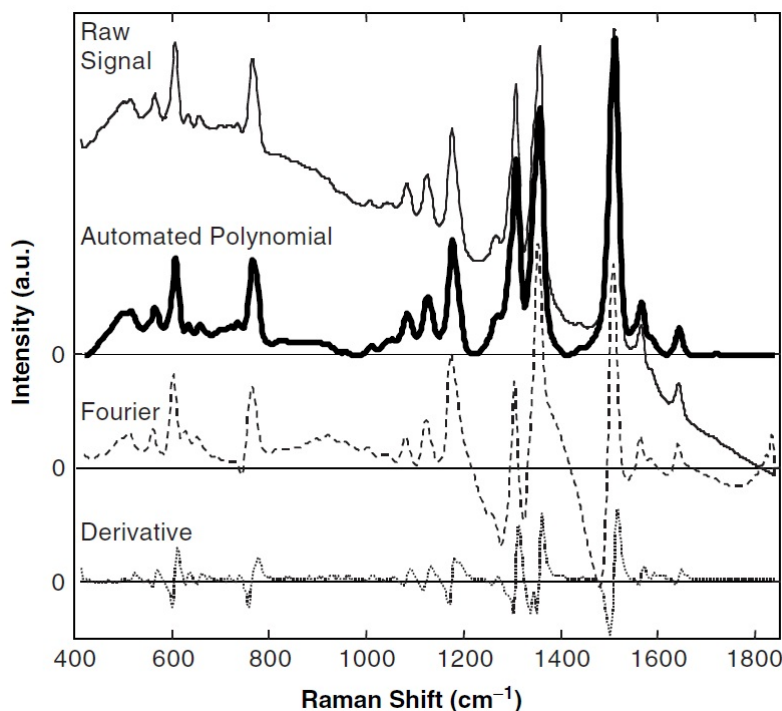


Figure 5: Comparison between automated polynomial, Fourier and derivative technique in fluorescence elimination. [3]

### 4.3 Analysis of Raman spectra

After pre-processing is done, the practical use of Raman spectra really begins. One of the advantages of Raman spectroscopy is the potential for automated clinical diagnosis. When we record a spectrum of a healthy and disease affected tissue, the differences in spectral features can be incorporated into diagnostic algorithms that classify the disease and set a diagnosis. An algorithm searches for differences in intensity, shape and location of the various known Raman bands that belong to certain molecules. The more information we get from the spectrum, the more accurate is the method of analysis and classification. Various techniques are used, such as neural networks and linear regression for classification, hierarchical cluster analysis (HCA), linear discriminant analysis (LDA) for disease differentiation, partial least squares, a regression-based technique and hybrid linear analysis for accurate extraction of concentrations of analytes, and many more [3].

The most important feature of Raman spectroscopy is that with all the information that a researcher gets, it brings answers to why a diagnosis for a certain disease can be made.

## 5 Clinical applications of Raman spectroscopy

There are several Raman active biological molecules in tissue that give distinctive peaks in the spectrum giving structural and environmental information about the tissue. The changes in tissue that occur as a result of a disease yield a characteristic Raman spectrum that can be used for diagnosis. Thus, everything from precancerous tissues to benign abnormalities can in principle be differentiated and detected.

Several in vivo tests have to be done, to fully evaluate the actual usefulness of Raman spectroscopy. Raman spectroscopy has been studied extensively for tissue diagnosis on skin, breast, esophagus, cervix, lung, throat, etc.

Besides Raman spectroscopy, several other optical techniques are being developed for the same applications, such as diffuse reflectance spectroscopy, fluorescence spectroscopy, photoacoustic and diffuse optical tomography. The main advantage of Raman spectroscopy is that tissue consists of many Raman active molecules, which have distinctive spectral signatures.

### 5.1 Skin cancer diagnostics

In general, skin consists of three layers. These are the superficial epidermis, dermis, and subcutis, the lower fatty tissue. The most important cells in the epidermis are keratinocytes and melanocytes, which produce the pigment of the skin. The dermis consists primarily of collagen and elastin which are produced by fibroblasts, and are responsible for support and elasticity of the skin. There are three common forms of skin cancer. The basal cell carcinoma (BCC), which accounts for in 75% of all skin cancers, squamous cell carcinoma (SCC), that is responsible for 20% of all skin cancers. Malignant melanoma accounts for about 4%, but causes about 77% of all deaths from skin cancer. In most cases, early diagnosis is critical for successful treatment of skin cancer.

Current diagnostic methods rely on physical examination with dermatoscope and skin biopsy. The first examination method is subjective and differs from dermatologist to dermatologist. Biopsy is very efficient, but is expensive, invasive, and time consuming. It becomes impractical if the patient has several suspicious lesions. There is a great interest in developing a non-invasive diagnostic tool that could reliably detect skin cancer in real time.

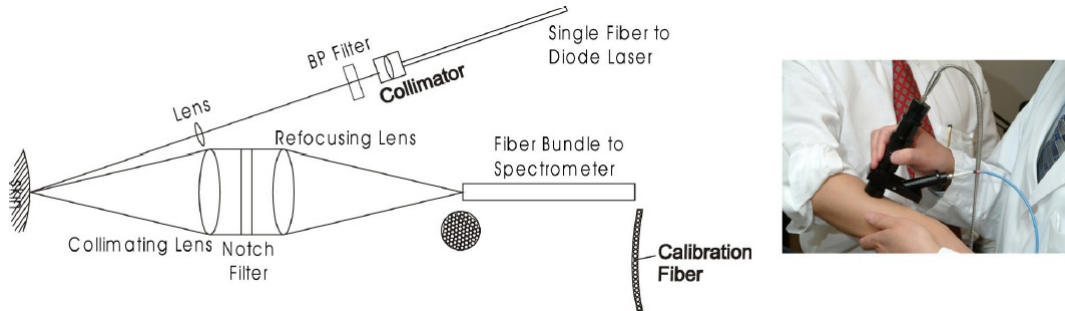


Figure 6: (Left) Optical layout of skin Raman probe used by Zeng et al. [6]  
(Right) A photograph of the probe in use.

The most known use of NIR Raman spectroscopy for in vivo skin cancer diagnosis was performed by Zeng et al. [6]. Their Raman spectroscopy setup consisted of a stabilized diode laser (785 nm), a specially designed Raman probe, transmissive imaging spectrometer and NIR optimized CCD (Fig. 6). There are 58 collection fibers and binning was used, which improved signal-to-noise ratio. Each spectrum was obtained within 1s. With this instrument they ana-

lyzed data from around 1000 skin lesions, including cancers.

The technique was identified as an alternative clinical tool to improve diagnostic specificity because of its ability to detect molecular changes associated with tissue pathology. The results showed that using this NIR Raman spectrometer, cancerous lesions could be differentiated from benign deformities with a sensitivity of 90% and specificity of 75%. Moreover, melanomas were differentiated from other pigmented structures with nearly 100% sensitivity and 70% specificity. (Sensitivity of a test indicates how many cases of a disease a particular test can find. Specificity of a test refers to how reliably it diagnoses a particular disease, without giving false-positive results.)

Silveira et al. [7] used similar instrumentation to obtain spectra of normal skin and basal cell carcinoma (BCC) in vivo. Fig. 7 compares two spectra obtained from normal skin and BCC. The peaks are mostly due to presence of proteins in the skin, such as actin, collagen and elastin, different lipids, nucleic acids, and hemoglobin. At first glance, the BCC skin has a similar biochemical constitution as normal skin. However, there are notable differences in the Raman peak intensities at  $800\text{-}1000\text{ cm}^{-1}$ ,  $1200\text{-}1400\text{ cm}^{-1}$ , and around  $1600\text{ cm}^{-1}$ . The team implemented a diagnostic model to discriminate BCC from normal skin using algorithms such as Principal Components Analysis (PCA) and Mahalanobis distance. They reported 85% accuracy in differentiating normal skin from BCC.

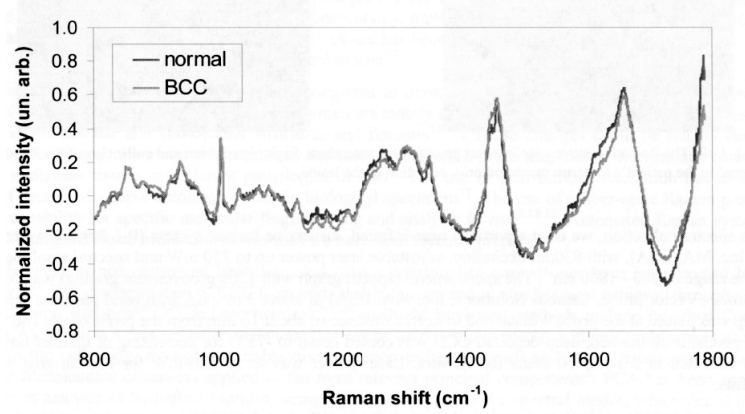


Figure 7: Raman spectra of normal and cancerous skin lesion acquired by Silveira et al. [7]

## 5.2 Breast cancer diagnostics

Breast cancer is one of the most common cancers in women. According to American Cancer Society a woman harbours a one-in-eight lifetime probability of developing breast cancer. The breast consists of mammary glands separated by fibrous connective tissue and a large amount of fatty tissue. There could be several benign changes in breast tissue such as ductal epithelial hyperplasia (DEH), fibroadenomas, fibrocystic changes, etc. However, the most dangerous are formations of malignant tumors. The most frequent invasive form of breast cancer is the infiltrating ductal carcinoma (IDC).

The most common technique for detecting breast cancer is mammography, which probes density changes in breast tissue with X-ray radiation. Because this is more of a screening technique rather than a diagnostic tool, there is around 70-90% chance that a lesion found by mammography is actually benign [9]. The ultimate diagnosis is biopsy. Breast biopsy is most often performed by surgical excision that removes the entire lesion or by a core needle that only removes a sample. Although biopsy is the most accurate method, it takes time and multiple

biopsies to make a complete diagnosis. Therefore, there is a desire of having a minimally invasive diagnostic technique, that gives results in real time.

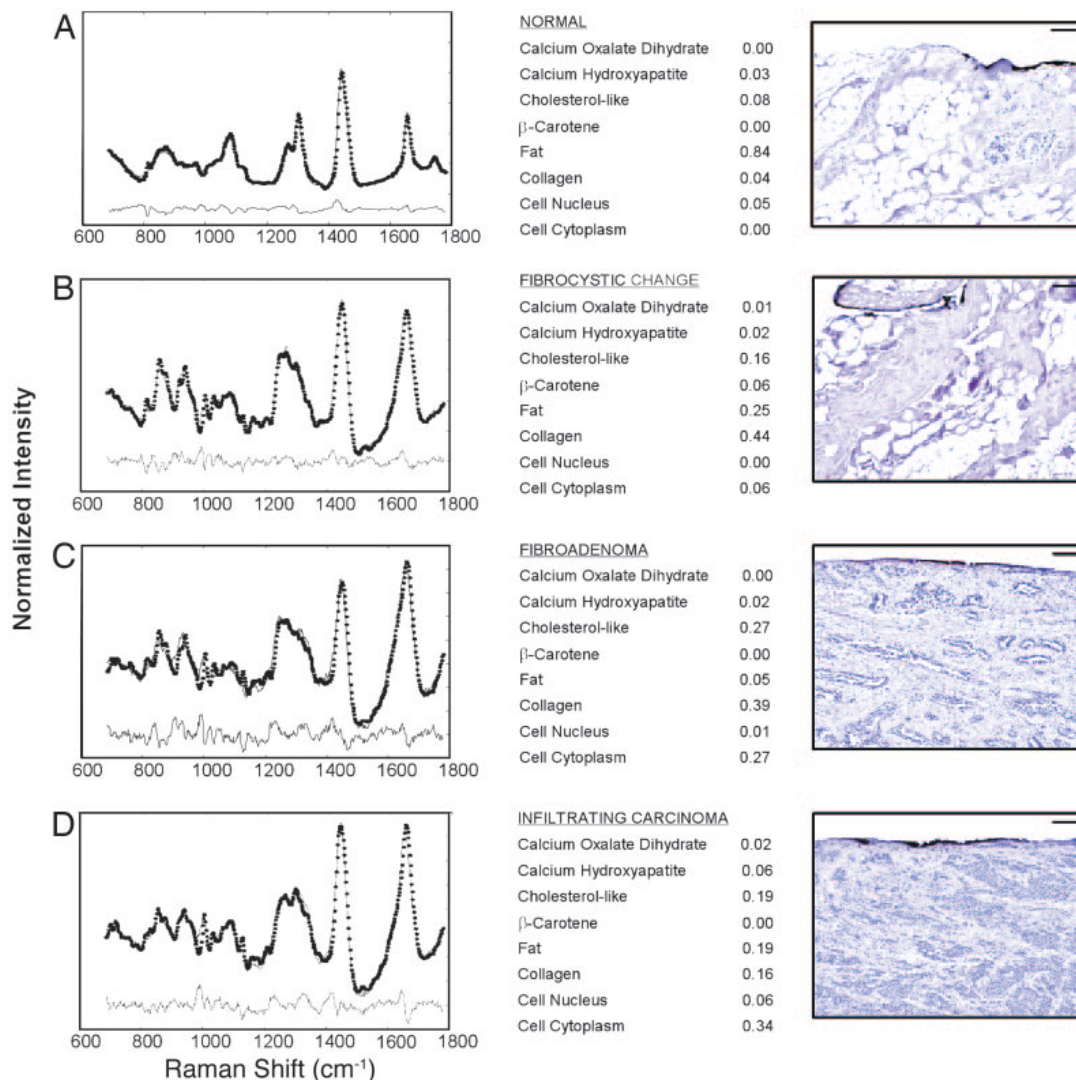


Figure 8: Normalized recorded Raman spectra (solid lines), model fits (dotted lines), residuals (grey line), fit coefficients, and tissue images. Black stained section of the tissue was used for histopathology in order to evaluate the diagnosis done by Raman spectroscopy. The scale bar is  $100 \mu\text{m}$ . (A) normal breast tissue, (B) fibrocystic change, (C) fibroadenoma, and (D) infiltrating carcinoma. [9]

Haka et al. [9] studied ex vivo samples of human breast tissue. Using a NIR Raman spectroscopy setup, they obtained spectra of normal tissues, benign lesions (fibrocystics changes, DEH and fibroadenomas) and malignant lesions (IDC). The group developed a Raman spectroscopic model that fits macroscopic tissue spectra with basis spectra derived from Raman microscopy of various breast tissue morphological structures. This model assumes that the Raman spectrum is a linear combination of spectra of its components and that signal intensity and chemical concentration are linearly related. The advantage of this model is that it takes into account the whole spectrum. Model fitting was performed by using a non-negativity constraint. The contribution of each basis spectrum resulted in a fit coefficient. The sum of the coefficients was normalized to one. So, the fit coefficients provide an insight into the chemical composition

of the tissue.

Fig. 8 shows normalized Raman spectra, model fits, and the residual (difference between the two spectra). It also contains fit coefficients corresponding to particular biochemical compounds. Fig. 9 shows a histogram of fit coefficients for better visualization of their relative changes in tissue pathologies. Normal breast tissue is primarily composed of fat, whereas abnormal breast tissues consist of a large amount of collagen and other characteristic compounds.

The group also developed a diagnostic algorithm that examines all of the data simultaneously. A discriminate analysis technique called logistic regression was used to correlate the normalized fit coefficients with the diagnostic categories for all morphological components included in the model. One result is shown on Fig. 10, where collagen content is plotted against that of fat. Each region corresponds to a certain type of tissue.

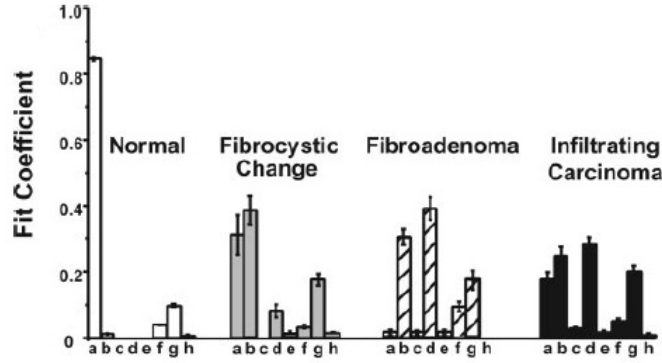


Figure 9: Histograms displaying the average composition of the measured tissue samples. fat (a), collagen (b), cell nucleus (c), epithelial cell cytoplasm (d), calcium oxalate (e), calcium hydroxyapatite (f), cholesterol-like (g), and  $\beta$ -carotene (h). [9]

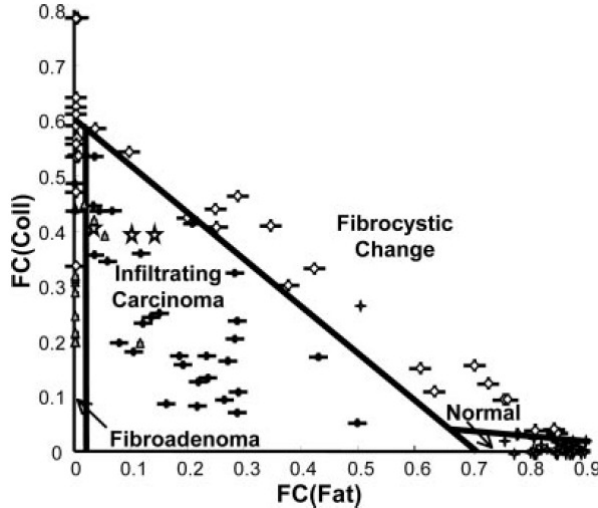


Figure 10: Scatter plot displaying the fat and collagen content for every spectrum obtained by Haka et al. Each region restricted by solid lines represents a certain type of tissue. [9]

An overall accuracy of 86% was achieved for detection of infiltrating carcinoma. The results of the study are very promising. The group is currently preparing the Raman spectrometer and algorithms for in vivo use, which will be the ultimate test for the technique.

## 6 Conclusion

Raman spectroscopy is a topic of continuous research in biomedicine. Its advantage is especially non-invasive nature, due to use of a low intensity laser beam. Although instrumentation for Raman spectroscopy is fairly simple, there is still room for improvement, especially in probe design and data analysis. Nevertheless, it could bring faster and more reliable diagnosis for cancerous changes in human tissue. Raman spectroscopy has already been preliminary tested and the results were very encouraging. This technique offers disease classification from biochemical composition and thus enables not only early and objective diagnosis, but also provides an insight into the involved disease process.

## References

- [1] [http://en.wikipedia.org/wiki/Raman\\_spectroscopy](http://en.wikipedia.org/wiki/Raman_spectroscopy) (May 2, 2012)
- [2] J.R. Ferraro, K. Nakamoto and C.W. Brown: *Introductory Raman Spectroscopy* (2nd ed., Academic Press, Boston, 2003)
- [3] T. Vo-Dinh: *Biomedical Photonics Handbook* (CRC Press, Boca Raton, 2003)
- [4] W. Demtröder: *Laser Spectroscopy* (3rd ed., Springer, Berlin, 2003)
- [5] H. Kuzmany: *Solid-State Spectroscopy* (2nd ed., Springer, Berlin, 2009)
- [6] H. Zeng, H. Lui and D.I. McLean: *Skin cancer detection using in vivo Raman spectroscopy*, SPIE Newsroom, DOI 10.1117/2.1201104.003705 (2011)
- [7] L. Silveira Jr., F. L. Silveira, M. T. T. Pacheco, R. A. Zângaro and B. Bodanese: *Diagnosing basal cell carcinoma in vivo by near-infrared Raman spectroscopy: a Principal Components Analysis discrimination algorithm*, Proc. SPIE, Vol. 8207 (2012)
- [8] A.S. Haka, Z. Volynskaya, M. Fitzmaurice, J. A. Gardecki, J. Nazemi, R. R. Dasari, R. Shenk, N. Wang and M. S. Feld: *Diagnosing breast cancer using Raman spectroscopy: prospective analysis*, J. Biomed. Opt., Vol. 14(5):054023 (2009)
- [9] A.S. Haka, K. E. Shafer-Peltier, M. Fitzmaurice, J. Crowe, R. R. Dasari and M. S. Feld: *Diagnosing breast cancer using Raman spectroscopy*, PNAS, Vol. 102, no. 35 (2005)
- [10] J.P. Motz: *Biomedical Raman Spectroscopy*, presentation at Harvard Medical School, <http://engineering.tufts.edu/bme/people/georgakoudi/> (May 22, 2012)